J. Phys. E: Sci. Instrum., Vol. 17, 1984. Printed in Great Britain

Rotating disc viscometer

L Bruschi, M Santini and G Torzo
Dipartimento di Fisica dell'Università di Padova and Gruppo Nazionale Struttura della Materia, Padova, Italy

Received 1 August 1983, in final form 29 September 1983

Abstract. A rotating disc viscometer, capable of performing accurate measurements in the critical region of a fluid, is described in this paper. This apparatus, developed in our laboratory, allows viscosity measurements to be performed with a very small fluid sample at the desired shear rate.

1. Introduction

The viscometer described in this paper has been developed in our laboratory to perform accurate viscosity measurements near the liquid–vapour critical point of fluids (Bruschi and Torzo 1983). We believe however that some interesting features of the device make it suitable to be used in many other situations. It is in fact a compact device without any external moving parts, and it can be easily thermoregulated at different temperatures. Only small fluid samples are needed, the volume filled by the fluid being only about 0.2 cm^3. Moreover the measurements can be performed at the desired shear rate.

The device consists essentially of a thin copper disc enclosed in a copper cylindrical cavity, filled with the fluid to be investigated (figure 1(*a*)). The disc is supported by a pivot and it can rotate around its symmetry axis. The angular velocity is measured by means of a light beam reflected by the disc surface. When a small black oxide spot on the disc surface crosses the light beam, the reflected intensity decreases, and a strong electric signal is observed at the output of an optical sensor. The time between successive spikes gives the rotational period θ.

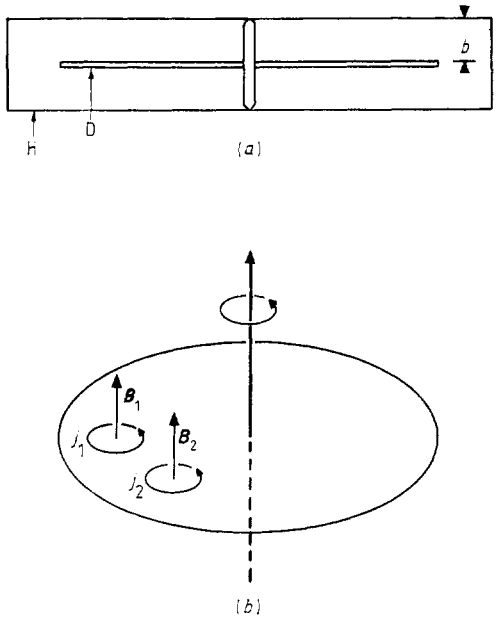

Figure 1. (*a*) Schematic view of viscometer: D, rotating disc; H, cylindrical housing; *b*, disc–housing surface gap. (*b*), Sketch of magnetic fields $\boldsymbol{B}_1$, $\boldsymbol{B}_2$, and of induced currents j_1, j_2 in the disc.

Small eddy currents are induced in the disc by two alternating magnetic fields $\boldsymbol{B}_1$ and $\boldsymbol{B}_2$ (figure 1(*b*)), generated by two coils. As a result of the interactions between magnetic fields and eddy currents the disc is forced to rotate, the working principle being the same as the one commonly used in mains power meters. The arrangement provides a driving moment τ_m, and a much smaller retarding moment τ_f. When the disc is in steady rotation we have

$$\tau_m + \tau_f + \tau_0 + \tau_\eta = 0 \tag{1}$$

where τ_0 is the frictional moment due to the bearings, and τ_η is the viscous moment. τ_η depends on the rotational period θ, on the fluid density ρ, and on the viscosity η

$$\tau_\eta = \tau_\eta(\theta, \rho, \eta). \tag{2}$$

The viscosity η can be measured if the viscous moment dependence, equation (2), is exactly known, and if τ_η can be measured, in steady rotation, through the measurements of τ_m, τ_f, and τ_0 (equation 1).

As, will be explained later, the viscous moment τ_η can be accurately calculated only when the boundary layer thickness $\delta = (\eta\theta/2\pi\rho)^{1/2}$ is either much smaller or much greater than the disc–housing gap b (figure 1(*a*)). Moreover the driving and retarding moments τ_m and τ_f in relationship (1) could be calculated only if the distribution of the eddy currents were accurately known. The viscous, driving, and retarding moments can only be estimated, so that this viscometer is not suitable for absolute measurements. However relative measurements can be accurately performed, after a careful calibration with a fluid of known density and viscosity.

2. Experimental method

Let us consider two alternating magnetic fields $\boldsymbol{B}_1$ and $\boldsymbol{B}_2$, orthogonal to the disc surface (figure 1(*b*)). They are produced by two coils driven by sine currents of the same frequency ν. Two current distributions are induced in the disc, the current densities j_1 and j_2 being a function of the position. At a particular place they are related to $\boldsymbol{B}_1$ and $\boldsymbol{B}_2$ by the relations

$$\begin{aligned} j_1 &= \alpha_1 \frac{\partial \boldsymbol{B}_1}{\partial t} + \alpha_1' \theta^{-1} \boldsymbol{B}_1 \\ j_2 &= \alpha_2 \frac{\partial \boldsymbol{B}_2}{\partial t} + \alpha_2' \theta^{-1} \boldsymbol{B}_2 \end{aligned} \tag{3}$$

where θ is the rotational period. The second term is due to the rotation of the disc and would be zero if the disc were blocked at rest. As a result of the interactions between the j_1 distribution and $\boldsymbol{B}_2$, and of the interactions between the j_2 distribution and $\boldsymbol{B}_1$, the disc is driven to rotate around its axis. The resultant driving moment could be calculated if one knew the fields and currents distributions. It depends on time and on the phase difference φ between $\boldsymbol{B}_1$ and $\boldsymbol{B}_2$. Summing up all the contributions, and averaging over one driving currents period ν^{-1}, we have

$$\tau_m \propto \nu B_{10} B_{20} \sin\varphi \tag{4}$$

where B_{10} and B_{20} are the amplitudes of the oscillating fields, and where numerical constants arising from the geometry of the set-up and from the electrical resistivity of copper have been disregarded.

In analogous way the interactions of j_1 with $\boldsymbol{B}_1$ and those

0022-3735/84/040312 + 05 $02.25 © 1984 The Institute of Physics

of j_2 with $\boldsymbol{B}_2$ produce a decelerating moment

$$\tau_f \propto -(\beta_1 B_{10}^2 + \beta_2 B_{20}^2)\theta^{-1}. \tag{5}$$

The small electromagnets producing $\boldsymbol{B}_1$ and $\boldsymbol{B}_2$ are made to have the same impedance Z, and therefore the phase difference φ between $\boldsymbol{B}_1$ and $\boldsymbol{B}_2$ is the same as that one between the driving voltages v_1 and v_2. Because τ_m has a maximum when $\varphi = \pi/2$, the coils are driven with two sine wave voltage v_1 and v_2 of the same frequency ν and with a phase difference $\varphi = \pi/2$. Letting the amplitudes v_{10} and v_{20} be equal, $v_{10} = v_{20} = v$, then $B_{10} \propto v$, $B_{20} \propto v$, and both τ_m and τ_f are proportional to v^2. Hence, if the exciting frequency ν and the phase difference φ are kept constant, relation (1) may be expressed as

$$\tau_\eta + \tau_0 + k_m v^2 - k_f \theta^{-1} v^2 = 0 \tag{6}$$

where k_m and k_f are constant factors.

Because τ_0 is constant, independent of ν and θ, it is convenient to express it through a constant voltage v_0

$$\tau_0 = -k_m v_0^2 \tag{7}$$

with the same k_m used for τ_m. Because both τ_η and τ_f reach a zero value as $\theta^{-1} \to 0$, v_0 represents the value of the exciting voltage below which the disc remains at rest.

A general hydrodynamic solution for τ_η is not available at present. We know it only in two limiting situations (Schlichting 1968), when the boundary layer thickness δ is much greater or much smaller than the gap b between the disc and the housing surfaces (figure 1(*a*)). The solutions are

$$\tau_\eta = -k\eta(\theta b)^{-1} \text{ for } \delta \gg b \tag{8}$$

$$\tau_\eta = -k'\eta(\theta\delta)^{-1} \text{ for } \delta \ll b \tag{9}$$

where k and k' are constants proportional to the fourth power of the disc radius r.

The above solutions are valid when the rotational period θ is sufficiently small to have $\delta \ll r$, but sufficiently great to avoid the onset of turbulent flow. This last condition imposes the Reynolds number $R = (r/\delta)^2$ to be smaller than a critical number $R_c \simeq 10^5$. To satisfy the mentioned conditions the rotational period must be such that

$$2\pi\rho r^2 \eta^{-1} \cdot 10^{-5} < \theta < 2\pi\rho r^2 \eta^{-1}. \tag{10}$$

The compressibility effects, present in a real fluid, can be neglected if the density changes $\Delta\rho$ are much smaller than ρ. Now $\Delta\rho$ is of the order of $\rho V^2/C^2$, where V is the fluid velocity and C is the sound velocity (Landau and Lifshitz 1959). This means that we must have $V^2 \ll C^2$. In our apparatus $V \simeq 2\pi r\theta^{-1}$, and the condition becomes

$$\theta^2 \gg (2\pi r/C)^2. \tag{11}$$

It is easy to show that the conditions (10), (11) are not difficult to be satisfied.

The constants k and k' which enter into the solutions (8) and (9) are not well known. They depend in a complicated way on the size and the geometry of the housing (Schlichting 1968). Also for a disc rotating in the above limiting situations an exact calculation of τ_η is not at hand, even if its dependence on η, θ, b and δ given by (8) and (9) is correct. It is therefore necessary to find an empirical expression for τ_η, performing measurements with a fluid of known density and viscosity.

To derive a general expression for τ_η, we assume it to have the following form

$$\tau_\eta = -k_0 \eta \theta^{-1} g(\delta) \tag{12}$$

where k_0 is a constant and $g(\delta)$ is an empirical function of the boundary layer thickness only. Combining equation (12) with (6) and (7), and rearranging the constants we get

$$\eta\theta^{-1} g(\delta) = A[(1 - c/\theta)v^2 - v_0^2]. \tag{13}$$

To obtain the empirical function $g(\delta)$ we observe firstly that in high vacuum $\eta = 0$ and therefore

$$\theta^{-1} = c^{-1} - (v_0^2/c)v^{-2}. \tag{14}$$

By measuring θ at various exciting voltages v and fitting the data with the linear relation (14) we get the values of the constants c and v_0. The constant voltage v_0 can also be measured, and more accurately, with a low density fluid. In this situation $\delta > b$, $g(\delta)$ assumes a constant value g_0 as shown by equation (8), and equation (13) may be written as

$$\theta^{-1} = A'(1 - c/\theta)v^2 - A'v_0^2, \tag{15}$$

where $A' = A/\eta g_0$. From measurements of θ at various values of v, the v_0 value can be easily obtained. Once the constants c and v_0 have been measured, the function $g(\delta)$ can be derived by measuring θ as a function of the density ρ in a fluid of known viscosity. The layer δ can be easily calculated from the known values of ρ and η, and $g(\delta)$ is obtained by fitting the data with the use of the relation (13). The function $g(\delta)$ should be valid for all fluids. Once the calibration has been performed, we may use the relationship (13) to get the viscosity of the fluid of interest, if we measure θ, ρ, and v.

The calibration of the viscometer is slightly temperature dependent, because the eddy currents depend on the electrical resistivity of copper. Now in usual conditions $c/\theta \ll 1$, and $v_0^2 \ll v^2$, and the RHS of equation (13) is about Av^2. In these conditions the temperature dependence of the calibration can be summarised by a temperature dependence of the constant A. This dependence can be easily found by calibrating the viscometer with the test fluid at various temperatures.

3. Experimental apparatus

The measuring cell is drawn in figure 2(*a*). A copper disc of 9 mm radius and 0.2 mm thickness can rotate around its symmetry axis inside a cylindrical housing of 10 mm radius and 0.8 mm height. The disc suspension is obtained by means of a steel pivot and two ruby bearings. The steel pivot is accurately positioned and soldered to the disc. The rubies are mounted on the housing. The vertical position of the upper ruby is adjusted by a small spring, as shown in figure 2(*b*).

The electromagnets M_1 and M_2 are made by 400 turns of 0.2 mm copper wire wound on a cylindrical iron core. The coils are externally shielded by cylindrical iron cups. The whole assembly is plugged inside the cell body and is separated from the fluid cavity by a final copper thickness. Radial slits are cut into this copper part to interrupt eddy currents (see detail C of figure 2(*a*)); the slits are filled with epoxy resin. The housing is finally lapped to get a flat smooth surface.

An optical glass window allows a light beam, emitted by a light emitter diode, to be reflected by the disc surface. The reflected beam is monitored by a phototransistor. The cell can be filled via a metal to metal needle valve built on the cell body. In this way the small fluid sample is entirely confined inside the test cavity. To avoid cell contamination by solid dust, the fluid is well filtered before entering the measuring cavity. The cell temperature is monitored by two NTC thermistors, and stabilised by a heater wound around the cell, driven by thermoregulation equipment. When a very good temperature stabilisation is needed, as in the measurements at the critical point, the cell can be mounted inside a multistage thermostat, as described elsewere (Bruschi 1982).

4. Electronics

The block diagram of the electronic apparatus is shown in

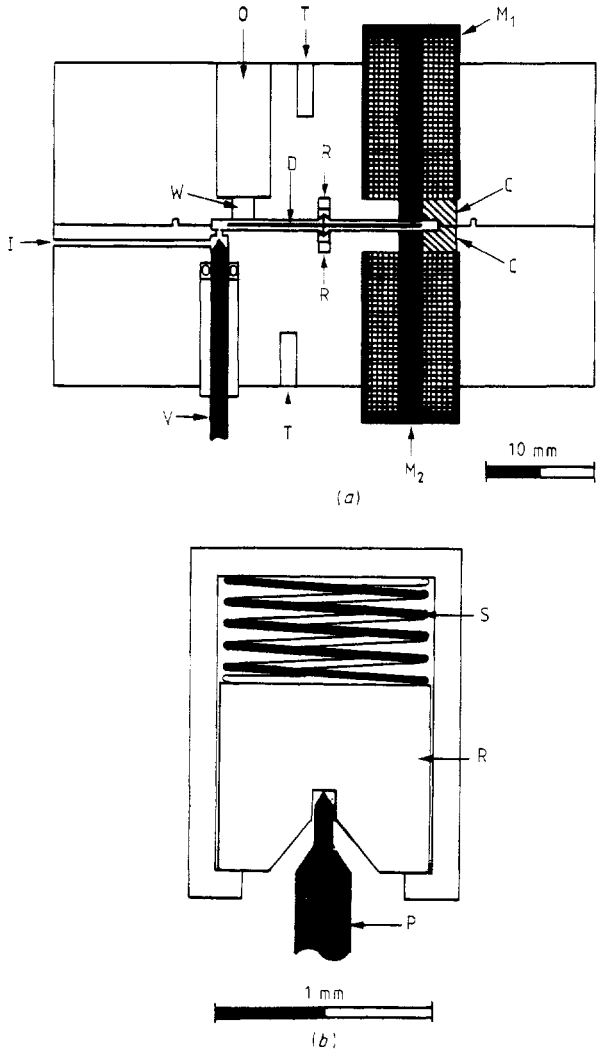

Figure 2. (*a*) Measuring cell: I, fluid inlet; V, needle valve; W, optical window; O, optical device; T, thermometers; D, rotating disc; R, rubies; $M_{1,2}$, electromagnets; C, vertical slits. (*b*), Ruby support: S, spring; R, ruby; P, disc pivot.

figure 3. The voltage-controlled oscillator VCO is a homemade, high amplitude stability oscillator (Bruschi *et al* 1981). It supplies, through the attenuator A_1, a sine wave voltage v_1 of the desired amplitude v to the electromagnet M_1. The electromagnet M_2 is driven by a quadrature sine wave v_2 obtained through the integrator I and attenuator A_2. The amplitude v of v_2 is set at the same value as the sine wave v_1. The frequency of the VCO oscillator is stabilised with the aid of a reference crystal oscillator CO($\nu = 1560$ Hz), and of a feedback loop involving the phase-sensitive detector PSD, as shown in the block diagram. In this way a very good amplitude and frequency stability is obtained. The frequency stability is as important as the amplitude stability, because the amplitude of the currents induced in the rotating disc and the amplitude of v_2 depend on the frequency as well as on the amplitude of VCO output. The amplitudes v_1 and v_2 remained stable to within 0.005% over periods of several days. The frequency stability is typical of crystal oscillators.

A standard optoelectronic device is used to monitor the angular velocity of the disc. A gallium arsenide infrared emitting diode (LED) was used as a light source. The bias current was about 8 mA. As a light sensor we used a silicon phototransistor, assembled with the LED in a plastic housing.

5. Experimental results

5.1. Calibration

Once mounted, the viscometer was degassed by pumping it for several days at a temperature of about 60 °C. Then the cell was filled with nitrogen gas at $T = 30$ °C and $P = 1$ atm ($\sim 1 \times 10^2$ kPa), and the disc was forced to rotate, under a constant driving voltage amplitude, to test the stability of the whole apparatus. Measurements were undertaken only when the angular velocity was stable to within 0.05% over several days.

The first set of measurements was performed at $T = 30$ °C in a vacuum of about 10^{-3} Torr (~0.133 Pa), by measuring the rotational period θ at various exciting voltage amplitudes v. The results are reported in figure 4 as θ^{-1} against v^{-2}. As explained in § 2 the dependence should be linear. The data lie in a restricted range of v^2, and thus the evaluation of the constants c and v_0 is not very accurate. The resulting value for c was $c = (1.44 \pm 0.07) \times 10^{-3}\ s^{-1}$. A better determination of v_0 was obtained by measuring θ, at the same temperature

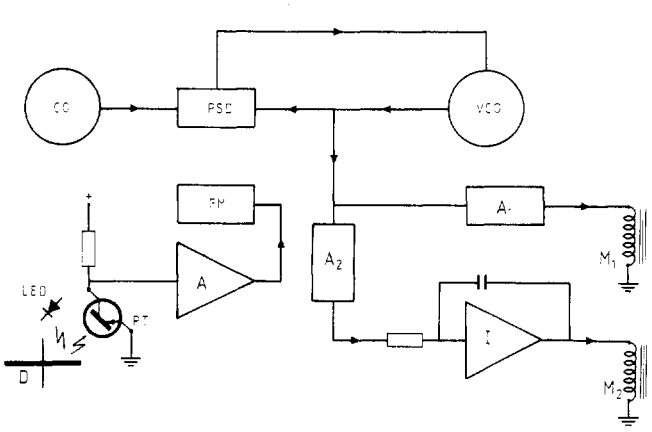

Figure 3. Block diagram of electronic apparatus: CO, crystal oscillator; PSD, phase-sensitive detector; VCO, voltage-controlled oscillator; $A_{1,2}$, attenuators; I, integrator; $M_{1,2}$, electromagnets; LED, light emitter diode; PT, phototransistor; A, amplifier; FM, frequency meter.

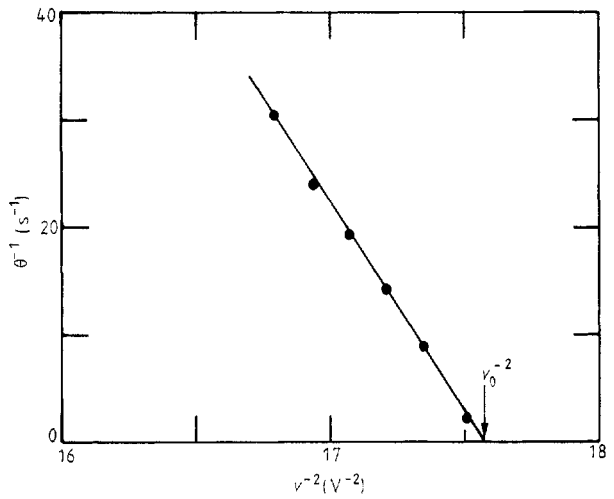

Figure 4. Period θ measurements in vacuum at 30 °C and at several values of exciting voltage v. The intercept with the v^{-2} axis gives the v_0^{-2} value.

$T = 30\,°C$, with nitrogen gas at $P = 1$ atm ($\sim 1 \times 10^2$ kPa). The measurements were taken at $\theta > 80$ ms. Assuming $\eta \simeq 180 \times 10^{-6}$ poise, and $\rho \simeq 1.13 \times 10^{-3}$ g cm^{-3}, we have $\delta > 4.5 \times 10^{-1}$ mm for the boundary layer thickness. Now $b = 3 \times 10^{-1}$ mm, and equation (15) may retained to be valid. The data are plotted in figure 5 as θ^{-1} against v^2. The constant v_0^2 turns out to be $v_0^2 = (5.65 \pm 0.03) \times 10^{-2}\ V^2$.

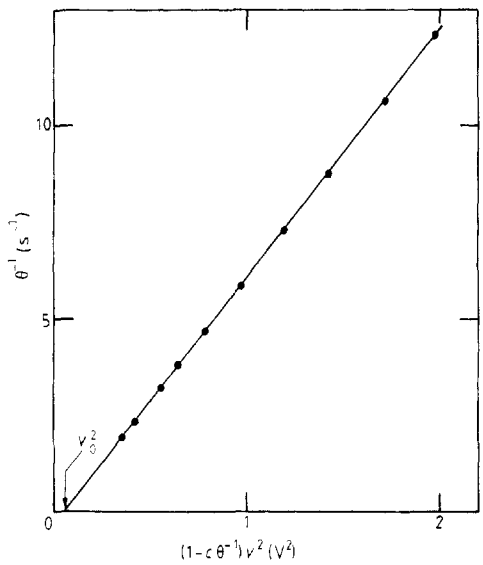

Figure 5. Measurements at 30 °C in nitrogen at 1 atm. The measured period θ is reported as θ^{-1} against $(1 - c\theta^{-1})v^2$. The straight line intercept with the $(1 - c\theta^{-1})v^2$ axis gives the v_0^2 value.

Finally, at the same temperature $T = 30$ °C, and at constant exciting voltages amplitude $v = 1.35$ V, we measured θ as a function of nitrogen pressure, in the range 1–80 atm.

The density ρ was calculated by using the state equation (Kestin *et al* 1971)

$$\rho = PM[RT(1 + D_1P + D_2P^2 + D_3P^3)]^{-1} \tag{16}$$

where the molecular weight $M = 28.014$ g, $R = 82.082$ atm cm^3/gK, $D_1 = -1.47 \times 10^{-4}$ atm^{-1}, $D_2 = 2.04 \times 10^{-6}$ atm^{-2}, $D_3 = 2.64 \times 10^{-9}$ atm^{-3}. ρ, P and T are expressed in g cm^{-3}, atm, K, respectively. The fluid pressure was measured by a gauge with an accuracy of about 2×10^{-2} atm. The nitrogen viscosity can be expressed as a function of density by the following relation

$$\eta = \eta_0 + \eta_1\rho + \eta_2\rho^2 \tag{17}$$

where $\eta_0 = 180.02\ \mu$P, $\eta_1 = 100.52\ \mu$P cm^3 g^{-1}, and $\eta_2 = 918.9\ \mu$P cm^6 g^{-2} (Kestin *et al* 1980). From the measured value of θ and P we calculated ρ through (16), η through (17), and finally boundary layer thickness δ. The data are reported in figure 6 as (η/θ) against δ. As predicted by solutions (8) and (9), the ratio (η/θ) results in a linear function of δ for low values of δ, while it saturates to a constant value at high values of δ. The data were fitted to relation (13) by using the following empirical function

$$g^{-1}(\delta) = d(1 + \delta/\delta_0) - \{2d - 1 + [1 - d(1 + \delta/\delta_0)]^2\}^{1/2}$$
$$d = d_0 + d_1[(\delta - \delta_0)^2 + d_2]^{-1} \tag{18}$$

where $\delta_0 = 1.331 \times 10^{-2}$ cm, $d_0 = 0.5046$, $d_1 = 2.56 \times 10^{-7}$ cm^2, $d_2 = 2.92 \times 10^{-5}$ cm^2.

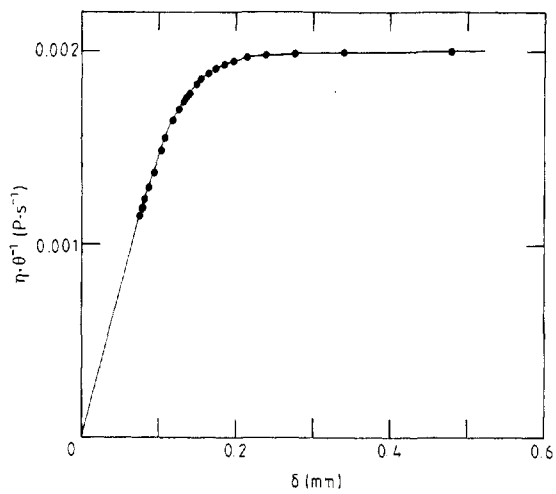

Figure 6. Calibration measurements in nitrogen at 30 °C and at several pressures. The experimental data are reported as $\eta \cdot \theta^{-1}$ against the boundary layer thickness δ (1 Ps^{-1} = 10^{-1} N m^{-2}).

The temperature dependence of the constant A was obtained measuring θ at constant density ($\rho = 1.13 \times 10^{-3}$ g cm^{-3}) at several temperatures ranging between 25 and 40 °C. By means of equation (13) and function (18) obtained at 30 °C, the values of the constant A at the same temperatures can be easily calculated. The calibrating values of nitrogen were obtained by equation (17). The temperature dependence of η_0 was calculated through a Keyes-type formula (Kestin and Whitelaw 1963)

$$\eta_0 = \alpha T^{1/2}[1 + (\beta/T)10 - \gamma/T]^{-1} \tag{19}$$

where $\alpha = 16.92\ \mu$P K$^{-1/2}$, $\beta = 286.3$ K, and $\gamma = 51.92$ K.

The experimental values of A can be fitted with a simple linear function of temperature

$$A(\mu\text{P s}^{-1}\text{ V}^{-2}) = 1.25761 \times 10^3 - 3.34067\ T(°C). \tag{20}$$

To show the accuracy of the calibration equations (13), (18) we report in figure 7 the quantity $(\eta/\eta' - 1)$ against the boundary layer thickness δ. The values of η have been calculated from the measured values of θ and ρ through the equations (13), (18). The η' are the calibrating values given by (17). As we can see the relative deviations are essentially within $\pm 0.1\%$.

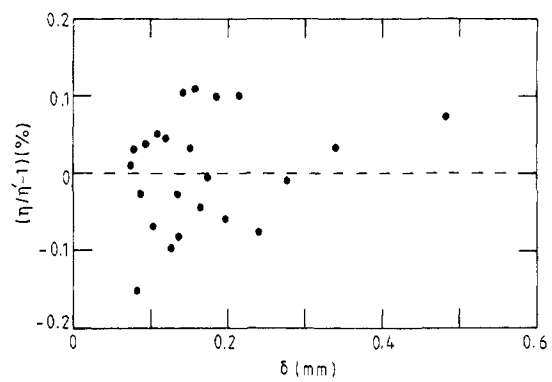

Figure 7. Relative deviations between the viscosity values η, obtained by means of the calibrating function, and the calibrating viscosity values η' of nitrogen at 30 °C, against the boundary layer thickness δ.

5.2. Viscosity measurements

To test the validity of assumption (12) and of the calibration performed with nitrogen gas, we measured the viscosity η in carbon dioxide at 31.63 °C, in the density range 2×10^{-3}–3×10^{-1} g cm^{-3}. The choice of this fluid was made to compare our results with the analogous one obtained by Kestin *et al* (1980) with the oscillating disc method. They also calibrated the viscometer against nitrogen at the same temperature and in the same pressure range as in the present work.

In table 1 we report the measurements performed with an exciting voltage of 1.35 V, as a function of density ρ. The CO_2 density was calculated from the measured pressure by using the state equation of Michels and Michels (1937). The η values are obtained from the measurements using the calibration performed with nitrogen gas.

Table 1. Experimental results for carbon dioxide at 31.63 °C ($1P = 10^{-1}$ N s m^{-2})

Density $\rho \times 10^3$ (g cm^{-3})	Period θ (ms)	Viscosity η (μP)	Smoothed values by Kestin *et al* (1980) η_s (μP)
1.945	76.84	152.08	152.26
3.552	77.60	152.18	152.33
5.354	79.07	152.24	152.42
18.49	97.41	152.66	153.17
28.50	109.87	153.35	153.89
44.70	126.38	154.91	155.37
75.28	150.32	158.61	159.28
90.32	160.30	161.21	161.75
120.75	178.40	167.36	167.92
168.69	203.32	178.38	—
208.68	223.25	191.36	—
240.21	239.32	204.98	—
275.46	256.53	220.31	—

Our results are shown in figure 8 together with those obtained by Kestin *et al* (1980). In table 1 we compare our data with the smoothed values η_s obtained in the density range 0–0.12 g cm^{-3} by the use of a density expansion proposed by Kestin *et al* (1980). The results agree to within 0.4%.

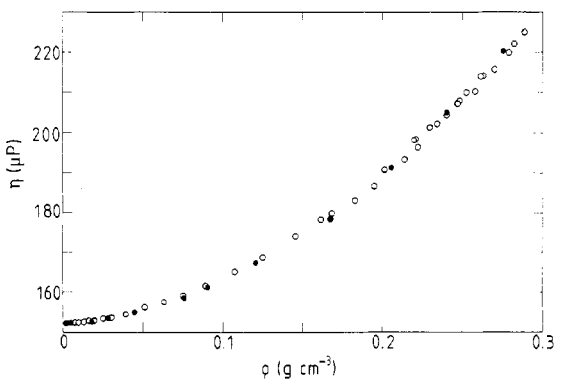

Figure 8. Viscosity η of carbon dioxide at several densities ρ: ●, this work; ○, Kestin *et al* 1980 ($1\ \mu P = 10^{-7}$ N s m^{-2}).

6. Conclusions

The viscometer described in this paper was developed in our laboratory to perform viscosity measurements in the critical region of fluids. In this particular situation one must measure at zero frequency (Bhattacharjee and Ferrell 1980) and the gravitational effects must be reduced as possible. The choice of a uniform rotating disc allows measurements in steady state condition while keeping the vertical thickness of the fluid sample within a very small value. The proposed calibration procedure follows essentially that previously used with the oscillating disc viscometer (Kestin *et al* 1980). With such a procedure, our viscometer has been used to measure the carbon dioxide viscosity in the critical region along the critical isochore (Bruschi and Torzo 1983). The critical temperature T_c has been approached down to $(T - T_c)/T_c \simeq 10^{-5}$. The results show a very good agreement with the existing theories on critical dynamics.

Acknowledgment

This work was supported by Ministero Pubblica Istruzione, Roma, Italy.

References

Battacharjee J K and Ferrell R A 1980 Dynamic scaling for the critical viscosity of a classical fluid
Phys. Lett. **76A** 290–2

Bruschi L 1982 Behaviour of shear viscosity near the critical point of carbon dioxide
Nuovo Cimento **1D** 361–81

Bruschi L, Storti R and Torzo G 1981 High-stability function generator
Rev. Sci. Instrum. **52** 125–8

Bruschi L and Torzo G 1983 Low frequency viscosity measurements near the critical point of carbon dioxide
Phys. Lett. **98A** 265–8

Kestin J and Whitelaw J H 1963 A relative determination of the viscosity of several gases by the oscillating disk method
Physica **29** 335–56

Kestin J, Paykoc E and Sengers J V 1971 On the density expansion for viscosity in gases
Physica **54** 1–19

Kestin J, Korfali Ö and Sengers J V 1980 Density expansion of the viscosity of carbon dioxide near the critical temperature
Physica **100A** 335–47

Landau L D and Lifshitz E M 1959 *Fluid Mechanics* (New York: Pergamon) p 91

Michels A and Michels C 1937 Series evaluation of the isotherm data of CO_2 between 0 and 150 °C and up to 3000 atm
Proc. R. Soc. **A160** 348–57

Schlichting M 1968 *Boundary-Layer Theory* (New York: McGraw Hill) pp 97 and 609